

Article

Protecting of Marble Stone Facades of Historic Buildings Using Multifunctional TiO₂ Nanocoatings

Mohammad A. Aldoasri ^{1,*}, Sawsan S. Darwish ², Mahmoud A. Adam ², Nagib A. Elmarzugi ³ 
and Sayed M. Ahmed ⁴

¹ National Nanotechnology Research Center, King Abdulaziz City for Science and Technology (KACST), P.O. Box 6086, Riyadh 11442, Saudi Arabia

² Department of conservation, Faculty of Archaeology, Cairo University, P.O. Box 12613, Giza 12221, Egypt; sawsansd@hotmail.com (S.S.D.); hafezm762000@yahoo.com (M.A.A.)

³ Faculty of Pharmacy, Tripoli University and National Nanotechnology Project, Biotechnology Research Center, LARST, P.O. Box 13100, Tripoli 00218, Libya; nelmarzugi@gmail.com

⁴ Ministry of Antiquities, The grand Egyptian Museum, P.O. Box 12556, Giza 12572, Egypt; sayedmansour32@yahoo.com

* Correspondence: aldosari@kacst.edu.sa

Received: 11 September 2017; Accepted: 26 October 2017; Published: 7 November 2017

Abstract: Stone surfaces and façades of historic buildings, due to their predominately outdoor location, suffer from many deterioration factors, including air pollution, soluble salts, relative humidity (RH)/temperature, and biodeterioration, which are the main causes of decay. In particular, the façades of the buildings deteriorate with direct exposure to these factors; deformation and disfiguration of superficial decoration and formation of black crusts are often observed on the stones. The development and application of self-cleaning and protection treatments on historical and architectural stone surfaces could be a significant improvement in the conservation, protection and maintenance of Cultural Heritage. A titanium dioxide nanoparticle has become a promising photocatalytic material, owing to its ability to catalyze the complete degradation of many organic contaminants and environmental factors. In this study, TiO₂ nanoparticles, dispersed in an aqueous colloidal suspension, were applied directly to historic marble stone surfaces, by spray-coating, in order to obtain a nanometric film over the stone surface. The study started with an investigation of some properties of TiO₂ nanoparticles, to assess the feasibility of the use of TiO₂ on historic stone and architectural surfaces. Scanning electron microscopy (SEM) was, coupled with energy dispersive X-ray (EDX) microanalysis, (SEM-EDX), in order to obtain information on coating homogeneity and surface morphology, before and after artificial aging; the activity of the coated surface was evaluated through UV-light exposure, to evaluate photo-induced effects. The changes of molecular structure occurring in treated samples were spectroscopically studied by attenuated total reflection infrared spectroscopy (ATR-FTIR); activity of the hydrophobic property of the coated surface was evaluated by Sterio microscopy, model Zeiss 2010 from Munich, Germany, equipped with photo camera S23 under 80X magnification. The efficacy of the treatments was evaluated through capillary water absorption, and colorimetric measurements, performed to evaluate the optical appearance. Results showed that TiO₂ nanoparticles are good candidates for coating applications on historic stone surfaces, where self-cleaning photo-induced effects are well evident; they enhanced the durability of stone surfaces toward UV aging, improved resistance to relative humidity (RH)/temperature and abrasion affect, reduced accumulation of dirt on stone surfaces when left in open air for 6 months, and did not alter the original features.

Keywords: photocatalysis TiO₂ nanocoating; historic buildings; historic stone façades; self-cleaning; artificial aging; colorimetric measurements

1. Introduction

The façades of historic buildings deteriorate with direct exposure to physical, chemical, and biological agents, which usually play an important role in the deterioration phenomenon [1,2]. The direct exposure of marble stone façades to these factors may affect, or even cause, physicochemical changes of the substrate, resulting in aesthetic deformation and disfiguration of superficial decoration, formation of black crusts and bio-geophysical and bio-geochemical damage [3,4]. In recent decades, there has been a strong impulse to develop innovative building materials that could offer extra value, in addition to outstanding mechanical properties and work-ability [5]. The use of nanotechnological solutions to better preserve historical and artistic items as well as architectural, monumental and archaeological elements is currently greatly increasing [6]. In the past few years, the building materials industry and conservation science have used the achievements of other sciences, such as physics, chemistry, geology and engineering [7]. There have been major developments in conservation science, colloids and interface science, together with materials science, which belong to the realm of popular nanosciences [8,9]. The latter area has attracted the conservation experts, due to the increasing loss of efficacy of conventional methods to achieve higher self-cleaning, surface protection, and consolidation efficiencies [10]. Nanomaterials, such as SiO₂ nanoparticles, CaCO₃ nanoparticles, clay nanoparticles, and Ca(OH)₂ nanoparticles, are some of the most common nanomaterials used in the consolidation of archaeological stone materials [11,12]. Silver nanoparticles, ZnO nanoparticles, and TiO₂ nanoparticles are the most common nanomaterials in the surface protection and preservation field [13,14]. Photocatalytic oxidation has a strong potential to be an effective process for removing and destroying low-level pollutants in the air [15]. Titanium dioxide is among the most important and widespread nanomaterials used in the building sector; TiO₂ is considered the most promising photocatalytic material for the degradation of environmental pollutants. It is nontoxic, highly efficient, and very stable under UV [16,17], relatively inexpensive, safe, chemically stable, highly photocatalytically active, compared with other metal oxide photocatalysts, compatible with traditional construction materials, such as cement, without making any original performance worse and effective under weak solar irradiation in an outdoor environment [18,19]. TiO₂ photoactivity is strongly influenced by the microstructure, presence and concentration of doping elements—the specific surface area and particle size [20]. In fact, the self-cleaning properties, consolidation and the transparency of nano-TiO₂ based materials could play a very important role for monuments, historical buildings and any other architectural surfaces exposed to environmental deterioration factors. The TiO₂-based coatings could potentially allow an easier maintenance of the original colour and aspect of the historical surfaces [21,22]. In addition it may be used as an additive in lime binder and consolidation polymeric materials, to improve the durability of lime-based mortars and other consolidation materials [23,24], and seems to allow the realization of transparent coatings that could improve the cleaning ability of historical surfaces, without changing their appearance properties, acting in a preventive and less invasive way to preserve their original aspect [25]. This may be due to the unique physical and chemical properties, size and the higher surface area of the nanoparticles.

In this study, TiO₂ nanoparticles, dispersed in an aqueous colloidal suspension were applied directly to historic marble stone, in order to obtain a nanometric film over the stone surface. The aim was to verify if this coating technology has self-cleaning and hydrophobic properties suitable for the restoration of stone materials belonging to our cultural heritage, and also to evaluate the ability to apply TiO₂ nanoparticles onto historic marble stone surface, determine whether there are any side effects of this material on stone surfaces and determine its chemical composition. For these purposes, and in order to evaluate the potential uses of TiO₂-based nanocoating, in the protection and consolidation of historic stone, different tests were carried out. In particular, the efficacy of the treatments on untreated, treated and treated aged samples—through the capillary water absorption test, the activity of the hydrophobic property of their coated surfaces and the ability to improve these coated surfaces against dirt accumulation—were evaluated by stereo microscopy for samples, after UV and thermal aging. On the other hand, surface morphology, before and after treatments, was examined

by scanning electron microscopy (SEM). Change in molecular structure occurring in treated samples, before and after aging, was studied by the Fourier-transform infrared spectroscopy-attenuated total reflection method (FTIR-ATR). Colorimetric measurement was performed to evaluate optical appearance. The improvement of stone mechanical properties was evaluated by abrasion resistance tests, to determine the abrasion resistance of natural stone.

2. Materials and Methods

2.1. Materials

2.1.1. Preparation of TiO₂ Nanocoating

A commercially-produced nanopowder of TiO₂ (with particle mean diameter <50 nm) were produced and characterized by Sigma Aldrich Company, Munich, Germany, data sheet supplied by the company. It consisted of a nanopowdered TiO₂ (anatase crystalline phase with particle mean diameter of <50 nm). Laboratory treatments were carried out using appropriate dilutions of the obtained TiO₂ nanopowder in an aqueous suspension of propan-2-ol. The alcohol medium was supplied by the Sigma Aldrich Company. The concentration of the treatment material is a crucial factor, since to obtain satisfactory results, the substrate must receive a suitable quantity of well-dispersed materials, in a sufficiently fluid form, and one of the important issues when choosing the concentration of the treatment material were the porosity and composition of stone material [26,27]. In addition, many other studies worked on the preservation of marble stone monuments, and recommended that—according to the stone nature and porosity and due to the very low porosity of marble stone—the proper concentration of treatment materials (2%) be appropriate, as the high content of nanoparticles led to aggregates of nanoparticles and low penetration inside the stone structure. When the nanoparticle content increased, they tended to form agglomerates that could be described as particles with higher dimensions (the obtained aqueous colloidal suspension having 2 wt % of TiO₂ content). Dispersions were subsequently stirred vigorously for 45 min [28–30].

2.1.2. Preparation of Experimental Marble Specimens

Carrara marble stone (with a porosity of about 1%), as one of the most common types of calcareous stones used for the monuments and decoration of history building façades, was used. The marble stone blocks were cut into cuboid samples (3 cm × 3 cm × 3 cm) for some tests, and cut into squared samples (10 cm × 15 cm × 3 cm) for other tests, such as the abrasion resistance test. The samples were washed with distilled water and dried in an oven at 105 °C for at least 24 h to reach constant weight. After that, they were left to cool at room temperature and controlled relative humidity (RH) 50%, then weighed again [31,32].

2.2. Methods

2.2.1. Application and Procedures of the Protection Nano-Coating on Stone Surface

The obtained TiO₂ aqueous colloidal suspension was applied to the marble stone samples through spray-coating with a spray gun with a 0.8 mm diameter nozzle. Spray-coating was selected because of its simplicity and compatibility with pre-existing surfaces [33]. Immediately before the application of the treatment material, the surface of the specimens was brushed, to remove any dust or other types of loose materials. Then, the substrates were pre-wetted with pure water, in order to allow proper application. The nano-coating was applied three times; treated samples were left for 1 month at room temperature and a controlled relative humidity (RH) of 50%. The treatment materials usually need some time, from 15 days to 1 month, in order to dry, and this depends on the stone type and the surrounding environmental conditions [34,35]. Some of the treated samples were submitted to investigation methods and the others were submitted to artificial aging and then to investigation methods, to monitor changes in protective materials after the accelerated aging test.

Untreated samples were used as references. Three samples were used for each series (treated and untreated). Stone treatments might ensure the homogenous distribution of the nanocoating on the surface of the stones, avoiding accumulation on the surface that hides the original colour characteristics. A further requirement of the protection treatments was a good penetration within the stone, in order to realize the adhesion of the inconsistent superficial layers with the unweathered stone beneath [36].

2.2.2. UV Aging Test

In order to evaluate the photo degradation effect of the coating and the stability of the hydrophobic property of the protective film, accelerated aging tests were performed through light emitted by a luminare C.T.S. Art lux 40 with 2 UV fluorescent tubes (5000 K, 45 cm long, 100 W, 220 V), with plexiglas protection screen, with a UV-A component, whose UV intensity was 2 w/cm^2 . The distance between samples and the light source was 20 cm. The samples were left under UV irradiation for 45 days [37], which was demonstrated in Figures 1 and 2, respectively.

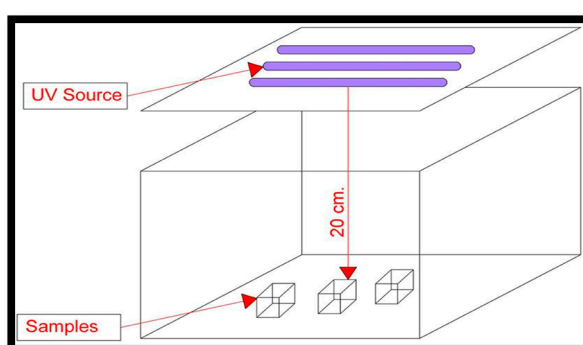


Figure 1. The samples exposed to the UV irradiation.

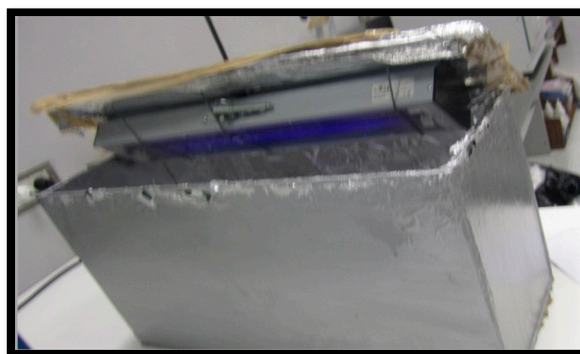


Figure 2. The samples inside the box under the UV source.

2.2.3. Artificial Aging Test (Wet-Dry Cycles)

This test was aimed at simulating actual environmental deteriorating conditions and quantifying the durability of the treatments. The artificial aging test was carried out by subjecting the treated samples to frequent changes in temperature and humidity, to find the effects of humidity and temperature on the rock, by trying to simulate the climatic change from sunny to wet, rainy weather. Thus, the treated samples were put in a temperature-controlled oven “Herous-Germany” on special frames. The test consisted of 30 cycles of immersion and drying as follows: 18 h of total immersion in distilled water, then 6 h in a temperature-controlled oven at $105 \text{ }^\circ\text{C}$ [38,39].

2.2.4. Dirt Accumulation Test

The stone samples were left in open air for 6 months, from February to July, and hung vertically on a wooden stand [40]. Table 1 shows the average temperature and relative humidity during every month.

Table 1. Average temperature (°C) during the dirt accumulation test in open air.

Month	February	March	April	May	June	July
Maximum temperature (°C)	23	25	27	30	32	35
Minimum temperature (°C)	10	12	15	19	19	21
Relative humidity (RH)	40	36	43	47	51	55

2.2.5. Morphological Analysis of the Stone Samples

The morphological characterization of untreated and treated stone surfaces was performed by scanning electron microscopy (SEM) Philips (XL30), equipped with an energy dispersive X-ray (EDX) micro-analytical system (the examination was carried out in SEM lab, Housing and Building National Research Center, Cairo, Egypt). The examinations were performed, in order to characterize and evaluate the surface morphology, the homogeneity, the behaviour and the distribution of the coating film after drying on untreated, treated and treated aged samples. The energy dispersive X-ray (EDX) micro analytical results were used to show the presence of TiO₂ locally spread on the surface of the treated marble. Images were acquired in backscattered mode (BSE).

2.2.6. Colorimetric Measurements

Evaluation of colour changes of the marble stone samples induced by application of the nanostructured remedial was carried out by colorimetric measurements, using a CM-2600d Kon-ica Minolta spectrophotometer, New York, United states of America (USA), to assess chromatic variations. In this process, chromatic values are expressed in the CIE L*a*b* space, where L* is the lightness/darkness coordinate, a* the red/green coordinate (+a* indicating red and −a* green) and b* the yellow/blue coordinate (+b* indicating yellow and −b* blue) [41].

2.2.7. Fourier Transformed Infrared Spectroscopy (ATR-FTIR)

The changes of molecular structure occurring in the treated samples upon ageing procedures were monitored by BRUKER'S VERTEX 70—attenuated total reflection infrared spectroscopy (ATR-FTIR spectrometer) in the 650–4000 cm^{−1} range, with a resolution of 4 cm^{−1}. The vibrational bands that appear in the infrared spectra provided information about the chemical functional groups of a sample which led us to study changes in characterization of the materials.

2.2.8. Mechanical Properties (Abrasion Resistance Test)

The Wide Wheel Abrasion (WWA) test is among the most widely used standard test methods for determining the abrasion resistance of natural stones. Marble samples that belong to calcareous metamorphic were tested for their abrasion resistance as well as physio-mechanical properties. Care was taken to select samples free of cracks and visible signs of weathering. The abrasion resistance of rocks was mainly controlled by their mineralogical and micro vs. macro textural characteristics. After precisely dimensioning the stone samples, according to the related testing procedures, the abrasion resistance of the considered stone types was determined in the laboratory, by using the Wide Wheel Abrasion test apparatus, in accordance with the procedures described in EN 14157 Standard (2004) (Natural Stones—Determination of Abrasion Resistance) [42].

Wide Wheel Abrasion (WWA) tests were applied on samples with dimensions of 10 cm × 15 cm × 3 cm. Samples used in WWA tests were dried at 105 °C for 24 h until they reached

a constant weight. The abrasive powder storage hopper was filled with dry powder and placed between the sample and an abrasive rotating disk (Figure 3). While the abrasive disk rotated at 75 cycles per minute, the flow of abrasivity was ensured to be uninterrupted. Two surfaces of each sample were exposed to the test. At the end of the test, the surface with traces of abrasion was examined under loupe and the borders of the abrasion area were depicted, as suggested in EN 14157 (2004). Following this step, three measurements were obtained from each abrasion surface, with a 0.01 mm precision digital caliper, and recorded. In the WWA experiments, it was important that the sample surfaces be smooth and parallel to each other, and before starting the experiments, the calibration of the apparatus was checked against a reference sample of “Boulonnaise Marble” [43].

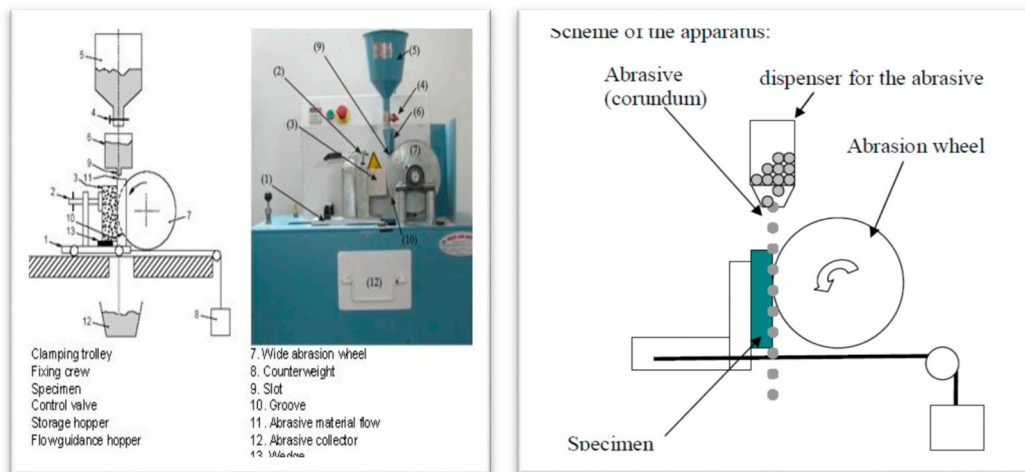


Figure 3. Wide Wheel Abrasion test device.

2.2.9. Water Absorption

The water absorption measurements were carried out using the gravimetric method [44]. The marble samples were completely immersed in deionized water at room temperature. After 24 h, the samples were taken out, wiped with tissue paper carefully and weighed immediately. The amount of absorbed water was calculated using the following equations:

$$\text{Density} = \frac{W}{V} = \dots \text{ gm/cm}^3$$

where W is Weight and V is Volume

$$\text{Porosity} = \frac{W_2 - W_1}{V} \times 100 = \dots \%$$

where W_1 is dry weight and W_2 is wet weight

$$\text{Water absorption} = \frac{W_2 - W_1}{W_1} \times 100 = \dots \% \quad (1)$$

Calculation of water absorption percentage, where W_2 is the mass of the sample after immersion in water for 24 h, and W_1 is the mass of the sample before immersion.

3. Results and Discussion

3.1. Characterization of Studied Historic Marble Samples

The investigation of historic marble samples is shown in Figure 4A. The total EDX analysis of the marble sample showed that calcium (Ca) is the dominant element; potassium (K), aluminum (Al), magnesium (Mg) and sulfur (S) were also observed. The XRD analysis (Figure 4B) showed that the marble sample consisted essentially of good type of fine calcite crystals as major mineralogical constituents, with trace amounts of halite.

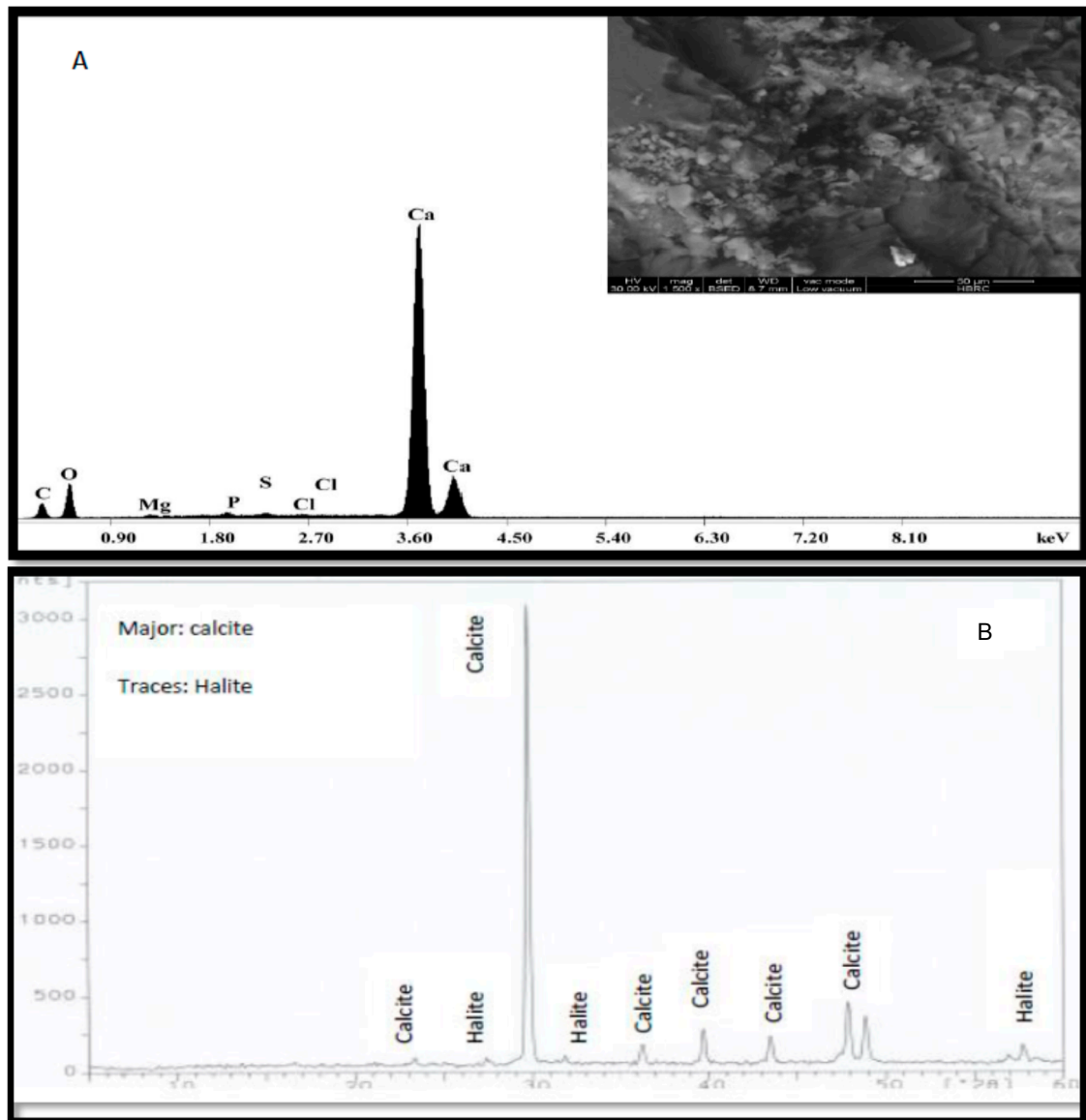


Figure 4. (A) Energy dispersive X-ray (EDX) spot analysis of historic marble samples; (B) XRD pattern of historic marble samples.

3.2. SEM/EDX Investigation

Scanning electron microscopy (SEM) observations were performed on treated, untreated and treated aged experimental marble samples; the SEM micrographs of the untreated sample (Figure 5a) show the homogeneous structure of the fine-grained calcite mineral, and the volume and distribution of the pores (marked with red circles), while the presence of some voids and disintegration was

noticed, because of the dissolving and disappearance of binding materials (marked with yellow circles). The SEM micrographs of the surfaces obtained after TiO_2 deposition (Figure 5b) show the coating film formed by a uniformly spread film on the marble surface. The micrographs also show that a coating film with a homogeneous and compact distribution (marked with white circle) which is crack-free, is generally observed, compared to the untreated ones. After UV aging, as shown in (Figure 5c), no significant changes were observed in the morphology of the protective film. Similar results were obtained for both samples, before and after solar radiation, which indicates that the coating film is stable under the effect of the artificial UV aging. This is due to the high photoactivity and unique physical and chemical properties of nano- TiO_2 . After artificial thermal aging (Figure 5d), small changes were observed in the coating film, and there were some fine cracks formed in the TiO_2 coating (marked with blue circles), but without any side effects on the film's uniformity and homogeneity.

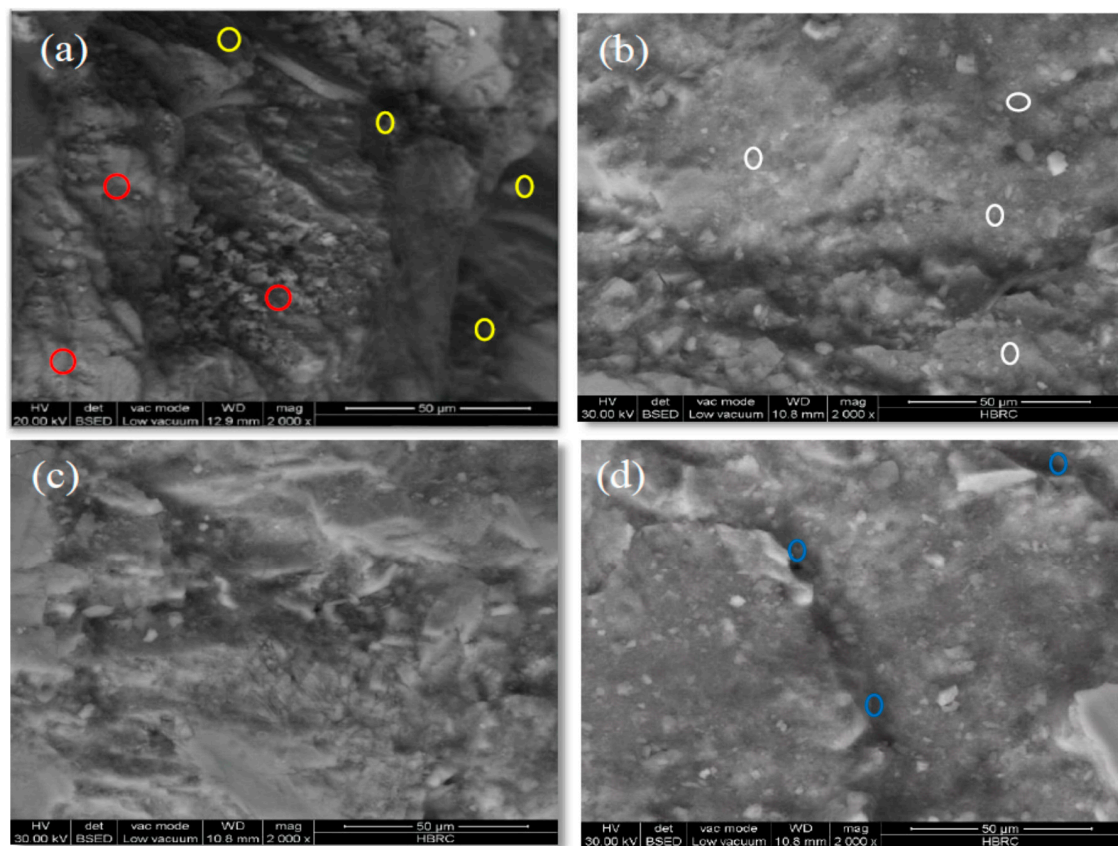


Figure 5. SEM images (2000 \times) of the experimental marble samples: (a) untreated; (b) treated; (c) treated samples after UV aging; and (d) treated samples after thermal aging.

The SEM tests were carried out on untreated samples, only before UV and thermal aging, because after aging, the material was too weak and no values could be reported. In addition to this, the evaluation tests in building material preservation were carried out on the treatment material to evaluate the behaviour of the coating material on the stone surface—not the stone material itself—to indicate if the coating film is stable under the effects of the artificial aging and deterioration factors.

In Figure 6, EDX spectra are reported, in order to show the presence of nano- TiO_2 , locally spread on the surface of the treated marble sample.

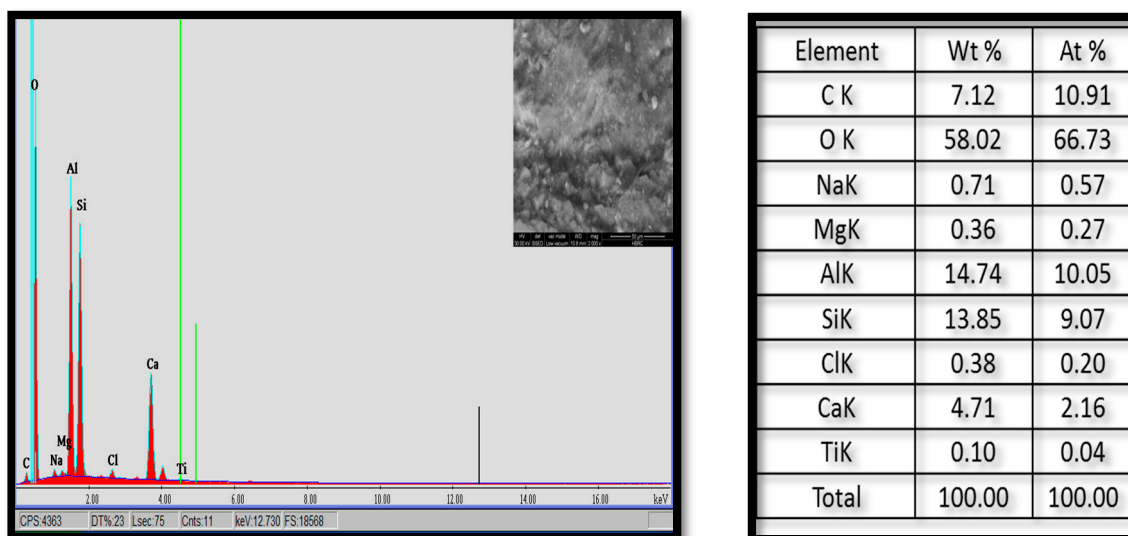


Figure 6. EDX spot of marble surface after the application of TiO₂ nano-coating.

3.3. Mechanical Properties (Abrasion Resistance Test)

The results of the abrasion resistance test are expressed by the width of the resulting groove in mm. Table 2 shows the average values for the abrasion resistance of experimental marble stone samples, before and after coating, and after thermal aging. In comparison, it was found that applying TiO₂ nanocoating to the stone surface increased its abrasion resistance value. After artificial thermal aging, the surface resistance was not affected too much and still gave the best result, compared to the untreated samples, as shown in Figure 7. This may be attributed to the role of nanoparticles in enhancing the durability of the stone surface and also improving the interaction with the stone grains, in addition to the superior physio-mechanical properties of TiO₂ nanoparticles.

Table 2. Results of the Wide Wheel Abrasion test.

Applied Protective Materials	Wide Wheel Abrasion Values (mm)
Untreated samples	19
Treated samples with TiO ₂ nano-coating	17.5
Treated samples with TiO ₂ nano-coating after thermal aging	18



Figure 7. Measurement of abrasion surface in the Wide Wheel Abrasion test: untreated (a); treated (b) and treated samples after thermal aging (c).

3.4. Effect of TiO₂ Nano-Coating on Dirt Accumulation

The effect of TiO₂ nanocoating on the accumulation of dirt and dust was investigated with a Stereo microscope. The experimental samples were divided into three types: untreated samples, treated samples, and treated samples after artificial aging. The samples were hung vertically on a

wooden stand and left in the open air for 6 months. Figure 8 shows that the accumulation of dirt was very high in untreated samples. After coating the samples with TiO₂ nanocoating, the accumulation of dirt and dust was reduced on stone surfaces. After artificial aging, no remarkable changes were observed in the surface's ability to reduce the accumulation of dirt, and the ratio of dirt accumulation on stone surface was less than in the untreated samples. Cleaning of the samples after treatment was very easy, using a soft brush, compared to the non-coated surfaces, where the dirt particles strongly adhered to the surface.

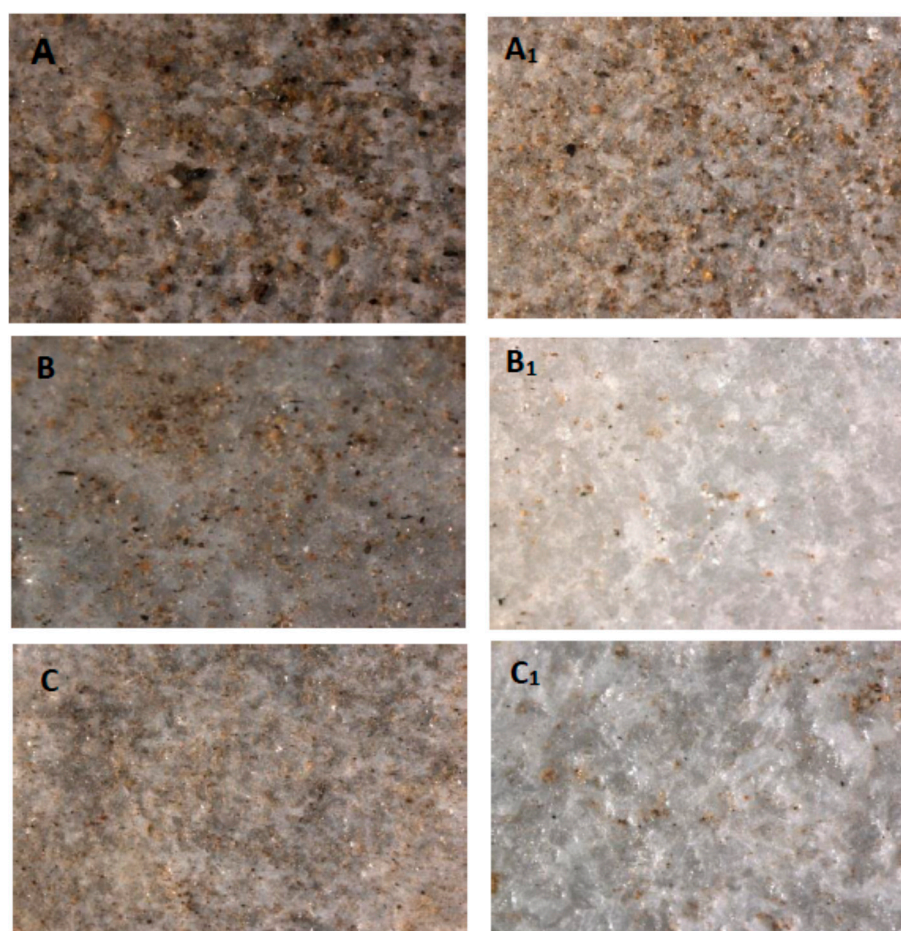


Figure 8. Stereo microscopy results from marble samples after being left in open air for six months (A,A₁) untreated samples before and after cleaning; (B,B₁) samples treated with TiO₂ nanocoating before and after cleaning and (C,C₁) samples treated with TiO₂ nanocoating after artificial thermal aging before and after cleaning.

3.5. Fourier Transformed Infrared Spectroscopy (ATR-FTIR)

The infrared spectra of marble stone show that calcite is the main mineral phase as observed at 1396.3, at 875, and at 712 cm⁻¹, assignable to the CO₃²⁻ group. TiO₂ nanoparticles showed absorptions at 1032.1 cm⁻¹ and at 1009.7 cm⁻¹, due to Ti-O-Ti vibrations. The spectra of the treated samples, before and after aging, in Figure 9, and the results listed in Tables 3 and 4, show that the intensities of the bands in the treated samples after thermal aging, decreased compared with that of standard samples, while no remarkable changes were observed in the treated samples exposed to U.V. radiation. On the other hand, after open air exposure, the intensity of the C=O group at 1396 cm⁻¹ sharply increased. Some researchers have shown that carbonate groups form as a result of CO₂ absorption on nano-TiO₂ surface [45,46]. These results were also confirmed by comparing the values of the relative

intensities of calcite, at 1396.3 cm^{-1} and of TiO_2 , at 1032.1 cm^{-1} and 1009.7 cm^{-1} , before and after aging. The values of the relative intensities decreased after thermal aging, were nearly the same after exposure to UV radiation and increased after open air exposure, compared with that of standard, completed data, as listed in Tables 3 and 4.

Table 3. FTIR-ATR spectra of the samples.

Wavenumber Range (cm^{-1})	Intensity (%)				
	Stone	Standard	Thermal Aging	UV Aging	Open Air
1394.0–1398.0	0.231	0.382	0.137	0.395	0.537
1030.0–1033.0	–	0.169	0.084	0.177	0.147
1008.0–1011.0	–	0.163	0.083	0.175	0.139

Table 4. FTIR-ATR spectra of the samples

Relative Intensity	Standard	Thermal Aging	UV Aging	Open Air
1396.3/1032.1	2.26	1.63	2.23	3.65
1396.3/1009.7	2.34	1.65	2.25	3.86

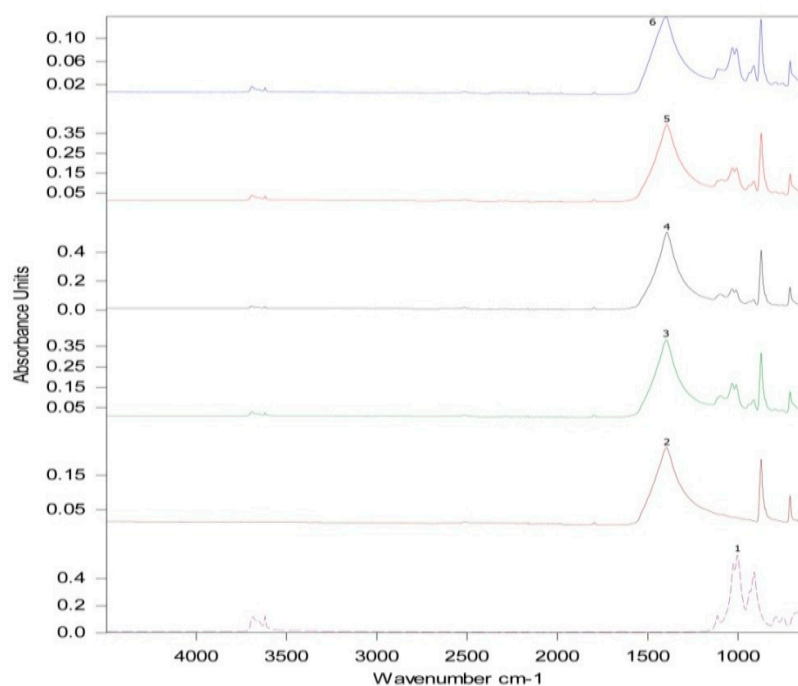


Figure 9. FTIR-ATR spectra of the samples, (1) TiO_2 nanopowders; (2) untreated surface; (3) treated surface; (4) after being left in open air for six months; (5) after thermal aging; and (6) after UV aging.

3.6. Colorimetric Test

Colour alteration was recorded before and after the coating applications and after artificial aging. The aim of this analysis was to determine whether the nanopowders could induce an increase in colour variation between the treated, untreated and the treated aged surfaces. The colour modification (ΔE) was calculated using the following equation:

$$\Delta(E) = \sqrt{\Delta L^* + \Delta a^* + \Delta b^*} \quad (1)$$

where ΔL^* , Δa^* and Δb^* represent the differences between the value of each chromatic coordinate in treated samples and the value in untreated ones. This parameter is important for aesthetic reasons,

since a coating should not induce ΔE^* greater than 5 [47,48], in order to preserve the original colour of surfaces. After treatment and aging, negligible colour variations were observed, (colour change with ΔE^* less than 5 is conventionally not visible to the naked eye). The average colour change caused by TiO_2 deposition was $\Delta E^* = 2.17, 3.06$ and 4.04 . This value is fully compatible with their use for architectural heritage, and more specifically, with the requirements of the maintenance field. The chromatic variation can be considered noticeable by human eye. The obtained data are fully listed in Table 5. According to Italian guidelines for the restoration of stone buildings, the ΔE value must be <5 ; other authors state that this threshold value should be <10 . The ΔE scale in stone materials conservation is as follows:

- $\Delta E < 0.2$: no perceivable difference;
- $0.2 < \Delta E < 0.5$: very small difference;
- $0.5 < \Delta E < 2$: small difference;
- $2 < \Delta E < 3$: fairly perceptible difference;
- $3 < \Delta E < 6$: perceptible difference;
- $6 < \Delta E < 12$: strong difference;
- $\Delta E > 12$: different colours.

Table 5. Color measurements for treated and aged samples.

Δ (Treated and Untreated Samples)				Δ (UV Aged and Untreated Samples)				Δ (Thermally Aged and Untreated Samples)			
ΔL^*	Δa^*	Δb^*	ΔE^*	ΔL^*	Δa^*	Δb^*	ΔE^*	ΔL^*	Δa^*	Δb^*	ΔE^*
2.03	0.41	0.66	2.17	2.89	0.41	0.92	3.06	3.82	0.35	1.27	4.04

3.7. Water Absorption

Water is one of the most important abiotic factors of decay in stone materials [49]. Once it penetrates into the pores by capillary force, water carries out its deteriorating effect through the chemical dissolution of the carbonate component of the stone, through physical phenomena such as freezing/thawing cycles, salt crystallization and through microorganism growth. For this reason, the hydrophobic property of the nanocoating products was tested by capillary absorption [50]. Density, porosity and capillarity water absorption were measured, in order to assess the decrease in wettability. Analyses were carried out on both untreated and freshly treated samples and after accelerated aging by UV radiation and thermal aging, to simulate coating behaviour after a certain period of solar irradiation, which may lead to a decreased water resistance due to alterations in the coating film. It is evident from the physical measurements that the treated samples were higher in bulk density. The efficiency of the nanocoating in the formation of a protective layer is shown from the reduction in water absorption and porosity, which can be referred to as the penetration of the nanoparticles into voids and pores, in addition to the photocatalytic and self-cleaning activities of TiO_2 nanoparticles. The hydrophobicity of the treated surfaces was tested again after UV aging. Treated surfaces seem to be not affected by solar radiation; no significant differences were observed in the behaviour of the samples after aging—which can be referred to as the photocatalytic activity of TiO_2 nanocoating—and they were stable under UV irradiation. After artificial thermal aging, negligible variations were observed, although behaviour was slightly different, but it was considered to be within the acceptable limit and did not affect the stone surface. The completed data are listed in Table 6.

Table 6. Average values of water absorption for treated and treated aged marble stone samples.

TiO ₂ Nanoparticles Concentration (2%)	Density (gm/cm ³)	Porosity (%)	Water Absorption (%)
Untreated sample	2.656	0.09	0.11
Treated sample	2.788	0.07	0.08
Treated sample after UV aging	2.788	0.07	0.08
Treated sample after thermal aging	2.666	0.09	0.09

4. Conclusions

In this study photocatalytic, hydrophobic and self-cleaning properties of an organic-TiO₂ nanocoating were tested. The aim was to examine the feasibility of using nano-TiO₂ based coating on historic marble stone surfaces in order to obtain a self-cleaning treatment, able to reduce deterioration effects. It is very evident that TiO₂ nanocoatings can effectively accelerate the degradation process of the dye under UV exposure and thermal aging. Hydrophobic measurements were performed before and after treatment, as well as after artificial aging. Results shown good water repellence after treatments and after aging; colour changes on the coated and uncoated stone showed negligible variations, before and after the application, and after artificial aging. The TiO₂ nanocoating enhanced the durability of the stone surface against an abrasion effect, and improved the mechanical properties of the marble stone surface. In addition, a nano-TiO₂ based coating enhanced the durability of stone surfaces toward UV aging, improved resistance to relative humidity (RH)/temperature, reduced the accumulation of dirt on stone surfaces when left in open air for 6 months, and did not alter the original features. This can be attributed to the compatibility and homogeneity between TiO₂ nanoparticles and stone building materials. The study confirmed that TiO₂ nanocoating can be considered a good candidate for coating applications on historic stone surfaces, where self-cleaning photo-induced effects are very evident.

Acknowledgments: The authors are much grateful to King Abdulaziz City for Science and Technology (KACST), Riyadh, Saudi Arabia for the valuable and continues scientific and moral support. The authors acknowledge the valuable assistance given by Merfat H. Khalil, the national center for housing and building research, and Yansuri Matsuda, (JICA), for their valuable technical support.

Author Contributions: Sawsan S. Darwish, Sayed M. Ahmed, and Mohammad A. Aldosari conceived and designed the experiments; Sayed M. Ahmed and Mahmoud A. Adam performed the experiments; Sawsan S. Darwish, Nagib A. Elmarzugi, and Mahmoud A. Adam analyzed the data; Mohamed A. Aldosari and Nagib A. Elmarzugi contributed reagents/materials/analysis tools; Sawsan S. Darwish and Sayed M. Ahmed wrote the paper.

Conflicts of Interest: The authors have no conflicts of interest to declare.

References

- Albertano, P. Deterioration of Roman hypogea by epilithic cyanobacteria and microalgae. In *Science and Technology for the Safeguard of Cultural Heritage in Mediterranean Basin*; CNR Editions: Palermo, Italy, 1995; Volume 2, pp. 1303–1308.
- El-Hady, A. Ground water and the deterioration of Islamic buildings in Egypt. In *The Restoration and Conservation in Islamic Monuments in Egypt*; Bacharach, J.L., Ed.; American University in Cairo Press: Cairo, Egypt, 1995; pp. 115–116.
- Crisci, G.M.; la Russa, M.F.; Macchione, M.; Malagodi, M.; Palermo, A.M.; Ruffolo, S.A. Study of archaeological underwater finds: Deterioration and conservation. *J. Appl. Phys. A* **2010**, *100*, 855–863. [[CrossRef](#)]
- Nugari, M.P.; Pietrini, A.M.; Caneva, G.; Imperi, F.; Visca, P. Biodeterioration of mural paintings in a rocky habitat: The Crypt of the Original Sin (Matera, Italy). *Int. Biodeterior. Biodegrad.* **2009**, *63*, 705–711. [[CrossRef](#)]
- Poon, C.C. Photocatalytic construction and building materials: From fundamentals to applications. *Build. Environ.* **2009**, *44*, 1899–1906.
- Quagliarinia, E. Self-cleaning materials on architectural heritage: Compatibility of photo-induced hydrophilicity of TiO₂ coatings on stone surfaces. *Appl. Surf. Sci.* **2013**, *14*, 1–7. [[CrossRef](#)]

7. Mamalis, A.G. Recent advances in nanotechnology. *J. Mater. Process. Technol.* **2007**, *181*, 52–58. [[CrossRef](#)]
8. Cessari, L.L.; Cenizia, B.; Elena, G.; Maria, G. Sustainable technologies for diagnostic analysis and restoration techniques: The challenges of the green conservation. In Proceedings of the 4th International Congress Science and Technology for the Safeguard of Cultural Heritage of the Mediterranean Basin, Cairo, Egypt, 6–8 December 2009.
9. Sekhar, P.; Ramgir, N.; Joshi, R.; Bhansali, S. Selective growth of silica nanowires using an Au catalyst for optical recognition of interleukin-10. *Nanotechnology* **2008**, *19*, 245502–245507. [[CrossRef](#)] [[PubMed](#)]
10. Matsunaga, T.; Namba, Y.; Nakajima, T. 751—Electrochemical sterilization of microbial cells. *Bioelectrochem. Bioenerget.* **1984**, *13*, 393. [[CrossRef](#)]
11. Dong, C.; Cairney, J.; Sun, Q.; Maddan, O.L.; He, G.; Deng, Y. Investigation of Mg(OH)₂ nanoparticles as an antibacterial agent. *J. Nanopart. Res.* **2010**, *12*, 2101–2109. [[CrossRef](#)]
12. Tsakalof, A.; Manoudis, P.; Karapanagiotis, I.; Chryssoloulakis, I.; Panayiotou, C. Assessment of synthetic polymeric coatings for the protection and preservation of stone monuments. *J. Cult. Herit.* **2007**, *8*, 69–72. [[CrossRef](#)]
13. Richards, R. *Surface and Nanomolecular Catalysis*; CRC Press: Boca Raton, FL, USA, 2006.
14. Ruffolo, S.A.; la Russa, M.F.; Malagodi, M.; Rossi, C.O.; Palermo, A.M.; Crisci, G.M. ZnO and ZnTiO₃ nanopowders for antimicrobial stone coating. *Appl. Phys. A* **2010**, *100*, 829–834. [[CrossRef](#)]
15. Nakata, K.; Fujishima, A. TiO₂ Photocatalysis: Design and applications. *J. Photochem. Photobiol. C Photochem. Rev.* **2012**, *13*, 169–189. [[CrossRef](#)]
16. Zhao, X.; Zhao, Q.; Yu, J.; Liu, B. Development of multifunctional photoactive self-cleaning glasses. *J. Non-Cryst. Solids* **2008**, *354*, 1424–1430. [[CrossRef](#)]
17. La Russa, M.F.; Ruffolo, S.A.; Rovella, N.; Belfiore, C.M.; Palermo, A.M.; Guzzi, M.T.; Crisci, G.M. Multifunctional TiO₂ coatings for cultural heritage. *Prog. Org. Coat.* **2012**, *74*, 1–6. [[CrossRef](#)]
18. Goffredo, G.B.; Munafò, P. Preservation of historical stone surfaces by TiO₂ nanocoatings. *Coatings* **2015**, *5*, 222–231. [[CrossRef](#)]
19. Graziani, L.; Quagliarina, E.; Bondioli, F.; D’Orazio, M. Durability of self-cleaning TiO₂ coatings on fired clay brick façades: Effects of UV exposure and wet & dry cycles. *Build. Environ.* **2014**, *71*, 193–203.
20. Munafò, P.; Goffredo, G.B.; Quagliarina, E. TiO₂ based nanocoatings for preserving architectural stone surfaces: An overview. *Constr. Build. Mater.* **2015**, *84*, 201–218. [[CrossRef](#)]
21. Ferrari, A.M.; Pini, M.; Neri, P.; Bondioli, F. Nano TiO₂ coatings for limestone: Which sustainability for cultural heritage. *Build. Environ.* **2015**, *71*, 193–203. [[CrossRef](#)]
22. Liu, Q.; Liu, Q.; Zhu, Z.; Zhang, J.; Zhang, B. Application of TiO₂ photocatalyst to the stone conservation. *Coatings* **2015**, *53*, 357–365.
23. Ruot, B.; Plassais, A.; Olive, F.; Guillot, L.; Bonafous, L. TiO₂-containing cement pastes and mortars: Measurements of the photocatalytic efficiency using a rhodamine B-based colorimetric test. *Sol. Energy* **2009**, *83*, 1794–1801. [[CrossRef](#)]
24. Franzoni, E.; Fregni, A.; Gabrielli, R.; Graziani, G.; Sassoni, E. Compatibility of photocatalytic TiO₂-based finishing for renders in architectural restoration: A preliminary study. *Build. Environ.* **2014**, *80*, 125–135. [[CrossRef](#)]
25. Karatasios, I.; Katsiotis, M.S.; Likodimos, V.; Kontos, A.I.; Papavassiliou, G.; Falaras, P.; Kilikoglou, V. Photo-induced carbonation of lime-TiO₂ mortars. *Appl. Catal. B Environ.* **2010**, *95*, 78–86. [[CrossRef](#)]
26. Tseripi, A.D.; Vlachopoulou, M.E.; Gogolides, E. Nanotexturing of poly(dimethylsiloxane) in plasmas for creating robust super-hydrophobic surfaces. *Nanotechnology* **2006**, *17*, 3977–3983. [[CrossRef](#)]
27. Manoudis, P.; Karapanagiotis, I.; Tsakalof, A.; Zuburtikudis, I.; Panayiotou, C. Super-hydrophobic polymer/nanoparticle composites for the protection of marble monuments. In Proceedings of the 9th International Conference on NDT of Art, Jerusalem, Israel, 25–30 May 2008.
28. Mansour, S. Comparative Study to Evaluate Efficiency of the Conventional Composites and Nano-Composites in Cleaning and Self-Protection for Some Archaeological Stone Surfaces. Applied on Selected Objects. Master’s Thesis, Conservation Department, Faculty of Archaeology, Cairo University, Giza, Egypt, June 2014.
29. Buasri, A.; Chaiyut, N.; Borvornchettanuwat, K.; Chantanachai, N.; Thonglor, K. Thermal and Mechanical Properties of Modified CaCO₃/PP Nanocomposites. *Int. J. Chem. Mol. Nucl. Mater. Metall. Eng.* **2012**, *6*, 1–4.

30. Eirasa, D.; Pessanb, L.A. Mechanical Properties of Polypropylene/Calcium Carbonate Nanocomposites. *Mater. Res.* **2009**, *12*, 517–522. [[CrossRef](#)]
31. Graziani, L.; Quagliarini, E.; Osimani, A.; Aquilanti, L.; Clementi, F.; Yéprémian, C.; Lariccia, V.; Amoroso, S.; D’Orazio, M. Evaluation of inhibitory effect of TiO₂ nanocoatings against microalgal growth on clay brick façades under weak UV exposure conditions. *Build. Environ.* **2013**, *64*, 38–45. [[CrossRef](#)]
32. Licciulli, A.; Calia, A.; Lettieri, M.; Diso, D.; Masieri, M.; Franza, S.; Amadelli, R.; Casarano, G. Photocatalytic TiO₂ coatings on limestone. *J. Sol-Gel Sci. Technol.* **2011**, *60*, 437–444. [[CrossRef](#)]
33. Enrico, Q.; Federica, B.; Giovanni, B.G.; Antonio, L.; Placido, M. Smart surfaces for architectural heritage: Preliminary results about the application of TiO₂-based coatings on travertine. *J. Cult. Herit.* **2011**, *13*, 1–6.
34. Bakr, A.M. Evaluation of the reliability and durability of some chemical treatments proposed for consolidation of so called-marble decoration used in 19th century cemetery (Hosh Al Basha), Cairo, Egypt. *J. Arab Archaeol. Union* **2011**, *12*, 75–96.
35. Helmi, F.M.; Hefni, Y.K. Using nanocomposites in the consolidation and protection of sandstone. *Int. J. Conserv. Sci.* **2016**, *7*, 29–40.
36. Manoudis, P.N.; Karapanagiotis, I.; Tsakalof, A.; Zuburtikudis, I.; Kolinkeová, B.; Panayiotou, C. Superhydrophobic films for the protection of outdoor cultural heritage assets. *Appl. Phys. A* **2009**, *97*, 351–360. [[CrossRef](#)]
37. Male, S.; Kolar, J.; Strlič, M.; Kočar, D.; Fromageot, D.; Lemaire, J.; Haillant, O. Photo-Induced Degradation of Cellulose. *Polym. Degrad. Stability* **2005**, *89*, 64–69. [[CrossRef](#)]
38. Lazzari, M.; Chiantore, O. Thermal-Ageing of Paraloid Acrylic Protective Polymers. *J. Polym.* **2000**, *41*, 6447–6455. [[CrossRef](#)]
39. Khallaf, M.K.; El-Midany, A.A.; El-Mofty, S.E. Influence of acrylic coatings on the interfacial, physical, and mechanical properties of stone-based monuments. *Prog. Org. Coat.* **2011**, *72*, 592–598. [[CrossRef](#)]
40. El-Feky, O.M.; Hassan, E.A.; Fadel, S.M.; Hassanb, M.L. Use of ZnO nanoparticles for protecting oil paintings on paper support against dirt, fungal attack, and UV aging. *J. Cult. Herit.* **2013**, *15*, 1–8. [[CrossRef](#)]
41. The International Organization for Standardization (ISO). *CIE Standard S014-4/E, Colorimetry. Part 4: CIE 1976 L*a*b* Colour Space*; ISO: Genève, Switzerland, 2007.
42. EN. EN 14157-2004 Natural Stones—Determination of Abrasion Resistance, European Standard—Wide Wheel Abrasion Resistance BS. Available online: <https://shop.bsigroup.com/ProductDetail/?pid=00000000030049570> (accessed on 25 October 2017).
43. Çobanolu, I.; Çelik, S.B.; Alkaya, D. Correlation between wide wheel abrasion (capon) and Bohme abrasion test results for some carbonate rocks. *Sci. Res. Essays* **2010**, *5*, 3398–3404.
44. UNI. *UNI 10859-2000 Cultural Heritage—Natural and Artificial Stones—Determination of Water Absorption by Capillarity*; Unifica Zione Italian (UNI): Rome, Italy, 2000.
45. Tumuluri, U.; Howe, J.D.; Mounfield, W.P.; Li, M.; Chi, M.; Hood, Z.D.; Walton, K.S.; Sholl, D.S.; Dai, S.; Wu, Z. Effect of Surface Structure of TiO₂ Nanoparticles on CO₂ Adsorption and SO₂ Resistance. *ACS Sustain. Chem. Eng.* **2017**, *5*, 9295–9306. [[CrossRef](#)]
46. Su, W.; Zhang, J.; Feng, Z.; Chen, T.; Ying, P.; Li, C. Surface Phases of TiO₂ Nanoparticles Studied by UV Raman Spectroscopy and FT-IR Spectroscopy. *J. Phys. Chem. C* **2008**, *112*, 7710–7716. [[CrossRef](#)]
47. Murray, M.D.; Darvell, B.W. Protocol for contact angel measurement. *Phys D Appl. Phys.* **1990**, *23*, 1150. [[CrossRef](#)]
48. NorMal, R. *Misure Colorimetriche Strumentali di Superfici Opache*. Available online: http://www.architettiroma.it/fpdb/consultabc/File/ConsultaBC/Lessico_NorMal-Santopuoli.pdf (accessed on 2 August 2017).
49. UNI. *UNI 10921-2001 Evaluation of the Efficacy of Water Repellent Treatments Applied on Stone Materials of Cultural and Artistic Interest*; Unifica Zione Italian (UNI): Rome, Italy, 2001.
50. Self-Cleaning Test Procedure (2007). Project Self-Cleaning Glass: Nano-Structured Self-Cleaning Glasses-Modelling and Laboratory Tests for Fundamental Knowledge on Thin Film Coatings, EC Normalisation and Customer Benefits. Available online: <http://cordis.europa.eu/project/rcn/74327en.html> (accessed 25 October 2017).

